TECHNICAL INFORMATION SERIES

R65SD27

MASS TRANSFER IN THE LOW REYNOLDS NUMBER VISCOUS LAYER AROUND THE FORWARD REGION OF A HYPERSONIC VEHICLE

L. GOLDBERG
S.M. SCALA

SPACE SCIENCES LABORATORY

MISSILE AND SPACE DIVISION

GENERAL ELECTRIC

SPACE SCIENCES LABORATORY

MASS TRANSFER IN THE LOW REYNOLDS NUMBER VISCOUS LAYER AROUND THE FORWARD REGION OF A HYPERSONIC VEHICLE

By

L. Goldberg
S. M. Scala

R65SD27
July 1965

MISSILE AND SPACE DIVISION

GENERAL ELECTRIC

CONTENTS

LIST OF FIGURES

ABSTRACT

This paper describes a theoretical investigation of the effect of mass transfer into the hypersonic low Reynolds number viscous layer upon the heat transfer rate and skin friction, and represents an extension of an earlier study by the present authors. New results have been obtained and correlated as a function of the Reynolds number. The range of applicability of the present fluid dynamic model is also discussed and comparisons are drawn with earlier work, both theoretical and experimental.

SYMBOLS

C_i	mass fraction of species i
C_{p_i}	specific heat of the i^{th} species at constant pressure
$\overline{C}_p$	frozen specific heat of mixture
$\mathcal{D}_{ij}$	binary diffusion coefficient
f	dimensionless stream function
h_i	static enthalpy of the i^{th} species, including chemical
h	static enthalpy of the mixture
$\overline{h}$	dimensionless enthalpy
K_B	curvature of body
P	static gas pressure
Q	heat transfer
$\mathcal{R}$	universal gas constant
R_B	body radius
T	temperature
u, v	velocity components
$\overline{u}$, $\overline{v}$	dimensionless velocity components
$\vec{v}$	macroscopic gas velocity
$\vec{v}_i$	absolute velocity of species i
$\vec{V}_i$	diffusion velocity of species i
V_∞	flight speed
$\dot{w}_i$	chemical source term, net mass rate of production of species i per unit volume by chemical reaction
x, y, r	coordinate system
γ	ratio of specific heats
δ_s	shock detachment distance

ϵ	density ratio across shock wave
η	transformed coordinate
μ	viscosity
ρ	density
τ	shear stress
$\underset{\sim}{\tau}$	stress tensor
$\varphi = \frac{X}{R_B}$	body coordinate angle

Subscripts

i	i^{th} species
s	behind shock
w	wall, surface of vehicle
∞	upstream, ambient conditions
η	denotes differentiation with respect to η

Dimensionless Groups

$$B = \frac{\dot{m}_w (H_s - h_w)}{Q_{wo}}, \text{ mass transfer parameter}$$

$$C_H = \frac{Q_w}{\rho_\infty V_\infty (H_s - h_w)}, \text{ Stanton number}$$

$$C_f = \frac{\tau_w}{1/2\, \rho_\infty V_\infty^2}, \text{ skin friction coefficient}$$

$$Le = \frac{\rho \bar{C}_p \mathcal{D}_{ij}}{K}, \text{ binary Lewis number}$$

$$Pr = \frac{\mu \bar{C}_p}{K}, \text{ Prandtl number}$$

$$Re_s = \frac{\rho_\infty V_\infty R_B}{\mu_s}, \text{ shock Reynolds number}$$

I. INTRODUCTION

For the controlled flight of slender ballistic re-entry vehicles and hypersonic lifting re-entry vehicles at high altitudes, it is mandatory that adequate information be available for the prediction and control of the exchange of mass, momentum and energy between the surface of the vehicle and its environment. Hypersonic flight in the Earth's atmosphere from the outermost regions down to the surface can, in principle, be treated and solved by utilizing kinetic theory and/or continuum mechanics. However, the problem is greatly simplified, if we suitably divide the entire regime into sub-regimes in which different aerothermodynamic phenomena dominate.

In Figure 1, the high altitude hypersonic flight regime is shown divided into sub-regimes most suitable to the present discussion (Ref. 1). Typical ballistic and lifting re-entry trajectories of hypersonic vehicles are superimposed. Note that Figure 1 is typical for a nominal nose radius equal to one tenth of a foot; for smaller nose radii, all of the low density effects are shifted to lower altitudes. Descriptive stagnation region velocity profiles are shown to the right of the respective flight regimes. These regimes are discussed below.

As is well known, hypersonic flight at low altitudes is associated with high Reynolds numbers and a flow field defined by a very thin shock wave followed by an influscid region separated from the body by a thin boundary layer. This is the ordinary hypersonic continuum regime, and the whole flow field is known as the shock layer. Conditions directly behind the shock wave are determined using the Rankine-Hugoniot relations and the influscid flow is determined by using one of the available hypersonic shock layer approximations (see, for example Ref. 2); e.g., modified Newtonian, or stream tube, in order to obtain outer boundary conditions for the boundary layer.

For suborbital flight speeds, the radiative heat transfer from the shock layer is very small compared with the aerodynamic heat transfer and hence the dominant energy, momentum and mass transfer processes can all be treated by studying the phenomena within the boundary layer adjacent to the surface. This procedure has yielded many useful solutions to the thermal protection problem, (e.g., Refs. 3-6).

At a somewhat higher altitude (lower Reynolds number) the fluscid effects extend throughout a major portion of the shock layer and the flow may no longer easily be separated into three distinct regions. Convention has now termed this flight region the hypersonic low Reynolds number flow regime which may be further divided as follows:

1) Viscous layer subregime - It is assumed that the classical conservation laws of macroscopic flow are applicable and the shock remains sufficiently thin to be treated as a discontinuity followed by at least a small influscid region.

2) Merged viscous flow subregime - At sufficiently low Reynolds numbers the thickened shock merges with the fully fluscid flow behind it, and the entire flow field from the free stream to the body surface should be treated as a single problem.

At extreme altitudes, (the free molecule flow regime) it is usually permissible to neglect collisions between incident and reflected molecules in studying interactions between the vehicle and its environment. However, it is vitally important that the state of the undisturbed gas (Ref. 7), and the surface-particle interactions (Refs. 8-10), be fully taken into account. With decreasing altitude, particles reflected from the surface begin interacting with the incident particles. It becomes necessary to utilize kinetic theory, e.g., the Boltzmann equation (Refs. 11-14) in order to obtain solutions in the near free molecule flow regime.

Between the low Reynolds number and near free molecule flow regimes, a transition regime exists in which the shock wave is formed requiring a more rigorous kinetic theory approach, (Ref. 15) possibly coupled with a macroscopic analysis in which higher order terms are introduced. It should be noted that the uncertainty in the extent of this region is indicated by the lightly shaded area plus the broken line in the velocity profile.

It is seen from Figure 1 that knowledge about the hypersonic low Reynolds number flow regime is important both for slender ballistic entry vehicles and lifting re-entry vehicles. The earliest studies, restricted to order of magnitude analyses, are summarized by Hayes and Probstein (Ref. 2) where the entire hypersonic flight regime is divided into seven subregimes from continuum to free molecule flow, including the boundary layer regime, vorticity interaction regime, viscous layer regime, incipient merged layer regime, fully merged layer and transitional layer regimes, first order collision theory regime and the free molecule flow regime. This classification scheme

has been the basis of most subsequent studies.

In Hoshizaki's study (Ref. 16) of the effect of bluntness-induced vorticity on the boundary layer, it was concluded that the inviscid momentum equations evaluated behind the shock are equivalent to using the vorticity as a boundary condition, and thus, the complete momentum equations incorporate the vorticity boundary conditions. Increases of the order of ten percent in heat transfer and skin friction were obtained when the vorticity terms were retained in the Navier-Stokes equations, as the Reynolds number was decreased to a minimum valid Reynolds number. However, these terms are retained in an appropriate low Reynolds number order of magnitude analysis. In Refs. 17-20, similar results were obtained by appealing to the low Reynolds number nature of the flow without special recourse to vorticity except as a modification of the pressure term.

In Refs. 16-19, the density was assumed constant through the shock layer. Since it can easily be shown that the variation of density through this shock layer is of the same order of magnitude as that across the shock wave, it would appear that the assumption of constant density is not realistic. In a more recent study (Ref. 20), the density variation was taken into account, and it was shown that as the Reynolds number decreases, the ratio of heat transfer calculated with density variation to the heat transfer calculated with constant density increases. Clearly, then, the variation of density across the viscous layer should be included in a theoretical model.

In all of the above studies however, solutions were obtained for the flow of a viscous non-dissociating perfect gas. Hence, these studies ignored the important physicochemical phenomenon of dissociation, which decreases the molecular weight of the gas and alters the relationship between density, temperature and pressure. Also not considered was the alteration in the flow produced by mass transfer from the surface, which was subsequently shown to have a considerable effect upon the structure of the viscous layer and other dependent variables, (Ref. 1).

In Ref. 17, Probstein and Kemp extended their analysis to the merged viscous layer problem by matching a simplified perfect gas shock structure solution with their constant density perfect gas viscous layer solution. More recently, Levinsky and Yoshihara, Ref. 21, also studied the merged viscous layer but included variable density.

Qualitatively, the latter results appear credible. However, in addition to the remarks made previously about the non-dissociating perfect gas model in the viscous layer solution, its use in the study of hypersonic shock wave structure in air is even more unrealistic, since not only is the gas within a hypersonic shock wave not in chemical equilibrium, it is not necessarily in thermodynamic equilibrium (Ref. 22) i.e., the relaxation times for the translation degrees of freedom are much shorter than the other degrees of freedom, (e.g., rotational, vibrational). In particular, the available kinetic energy of the molecules is redistributed among many different internal modes of energy storage which absorb energy at different rates, but nevertheless in parallel processes and not in series. It is stressed that the dissociation and ionization processes which absorb energy and act to reduce the gas temperature, will begin before thermal equilibration is complete.

Cheng (Ref. 23) examined the merged viscous layer without recourse to the weak approximation of a perfect gas shock wave structure. Instead as suggested by Sedov, et. al. (Ref. 24) the Rankine-Hugoniot shock relations were modified by assuming first order corrections to account for heat conduction and the normal component of momentum transfer due to the viscous effects in the shock wave. With this approach, he has apparently been able to extend the perfect gas low Reynolds number viscous layer analysis out to almost the perfect gas near free molecule results of Willis (Ref. 14).

The present analysis has been carried out in the regime defined in Figure 1 as the hypersonic low Reynolds number viscous layer regime. In this regime, the viscous layer thickness δ is significant compared to the shock detachment distance δ_s, but $\delta/\delta_s < 1$, and the shock wave thickness is assumed to be sufficiently small so that it can be assumed that the flow is in thermochemical equilibrium behind the shock, before entering the viscous layer.

The governing equations utilized in the analysis are the equations of change for the flow of a compressible chemically reacting gas. Included are the conservation of mass, momentum and energy. In order to simplify the system of equations, the diffusion equations were uncoupled by assuming a Lewis number of unity. The boundary conditions are split; some are specified at the surface and the others behind

the shock wave.

To evaluate the remaining transport coefficients, the Prandtl number was assumed to be constant at a value of 0.71 and Sutherland's law was utilized for calculating the viscosity of dissociated air.

Even after expanding the simplified version of the governing equations into the usual body-oriented coordinates, it is necessary to make further simplifying assumptions in order to reduce the system of equations to a more tractable form. It is further assumed that the shock layer thickness δ_s is small compared with a characteristic dimension of the vehicle, in this case the nose radius, R_B. In fact, it has been shown, e.g., Refs. 1, 2, 20, 25, that

$$\frac{\delta_s}{R_B} = O(\epsilon) \tag{1}$$

in the stagnation region of a hypersonic vehicle. Based on this assumption, the order of magnitude of each term in the expanded governing equations may be calculated. Retaining all terms from order one to those of order $(Re_s)^{-1}$ yields the equations appropriate for a low Reynolds number analysis. Utilizing the method of separation of variables, the four non-linear partial differential equations are reduced to a tenth order set of six non-linear ordinary differential equations with split boundary conditions. The primary additional assumptions are: 1) the shock is concentric with the body, and 2) the variables are separable. The resulting system of equations and boundary conditions is then utilized to obtain first order non-similar solutions to the flow field in the forward region of the hypersonic low Reynolds number viscous layer.

II. BASIC RELATIONS

The utility of the macroscopic conservation equations which lead to the boundary layer equations in the high Reynolds number continuum regime has been amply demonstrated over the past fifty years. In extending the analysis to lower Reynolds numbers, it is assumed that the density is sufficiently large that the same initial macroscopic governing equations are applicable. In the absence of external force fields the steady state form of these equations is:

Conservation of Species i

$$\nabla \cdot (\rho_i \vec{V}_i) = \dot{w}_i \tag{2}$$

Conservation of Momentum

$$\rho (\vec{V} \cdot \nabla) \vec{V} = - \nabla p + \nabla \cdot \underset{\sim}{\tau} \tag{3}$$

Conservation of Energy

$$\rho \vec{V} \cdot \nabla \left(h + \frac{\vec{V} \cdot \vec{V}}{2}\right) = - \nabla \cdot \vec{Q} + \nabla \cdot (\underset{\sim}{\tau} \cdot \vec{V}) \tag{4}$$

Equation of State

$$\rho = \rho (h, p) \tag{5}$$

Summation over all species in equation (2) yields the global continuity equation

$$\nabla \cdot (\rho \vec{V}) = 0 \tag{6}$$

Implicit in the above definitions is that the gaseous system is composed of a mixture of chemically reacting perfect gases. Upon neglecting the Dufour effect and the transportof radiative energy, the heat flux vector $\vec{Q}$ is (Ref. 26),

$$\vec{Q} = - k \nabla T + \sum_i \rho_i \vec{V}_i h_i \tag{7}$$

i.e., the sum of the Fourier conduction and the energy transferred by diffusion. From the definition of h, it is seen that

$$\nabla T = \frac{1}{\overline{C}_p} \left[\nabla h - \sum_i h_i \nabla C_i\right] \tag{8}$$

where $\overline{C}_p$ is the frozen specific heat:

$$\overline{C}_p = \sum_i C_i C_{p_i} \tag{9}$$

As a first approximation, it is assumed that the gaseous components with similar

thermal and chemical behavior may be treated as a single averaged component so that the sum total can be treated as a binary mixture of "air atoms" and "air molecules". Then, neglecting pressure and thermal diffusion effects, the mass flux with respect to the mass-averaged velocity reduces to the classical Fick's diffusion relation

$$\rho_i \vec{V}_i = - \rho \mathcal{D}_{ij} \nabla C_i \tag{10}$$

Substitution of eqs. (8) and (10) into (7) yields

$$\vec{Q} = - \frac{\mu}{Pr} \left[\nabla h + (Le-1) \sum h_i \nabla C_i \right] \tag{11}$$

Assuming a Lewis number of unity thus yields

$$\vec{Q} = - \frac{\mu}{Pr} \nabla h \tag{12}$$

and the diffusion equations(2) are uncoupled, even for the case of non-equilibrium flow, without resorting to any specific constraint on the chemical source term, i.e., the term $\sum_i \dot{w}_i h_i$ is accounted for implicitly.

With these simplifying assumptions the governing equations valid in the low Reynolds number regime appear expanded below for the coordinate system shown in figure 2.

Continuity:

$$\frac{\partial}{\partial x} (\rho u r^j) + \frac{\partial}{\partial y} (\rho v r^j) + K_B r^j \rho v = 0 \tag{13}$$

x-Component of Momentum:

$$\rho \left[u \frac{\partial u}{\partial x} + v \frac{\partial u}{\partial y} + K_B uv \right] = - \frac{\partial p}{\partial x} + \frac{\partial}{\partial y} \left[\mu \frac{\partial u}{\partial y} \right] + K_B \left[(2+j) \mu \frac{\partial u}{\partial y} - \frac{\partial}{\partial y} (\mu u) \right] \tag{14}$$

y-Component of Momentum:

$$\rho \left[u \frac{\partial v}{\partial x} + v \frac{\partial v}{\partial y} - K_B u^2 \right] = - \frac{\partial p}{\partial y} + \frac{4}{3} \frac{\partial}{\partial y} \left[\mu \frac{\partial v}{\partial y} \right] + \frac{\partial}{\partial x} \left[\mu \frac{\partial u}{\partial y} \right] + j \frac{\mu}{r} \frac{\partial u}{\partial y} - \frac{2}{3} \frac{\partial}{\partial y} \left[\mu \left(\frac{\partial u}{\partial x} + j \frac{u}{r} \right) \right] \tag{15}$$

Energy:

$$\rho\left[u\frac{\partial}{\partial x}\left(h+\frac{u^2}{2}\right)+v\frac{\partial}{\partial y}\left(h+\frac{u^2}{2}\right)\right]=\frac{\partial}{\partial y}\left(\frac{\mu}{Pr}\frac{\partial h}{\partial y}\right)$$
$$+(1+j)K_B\frac{\mu}{Pr}\frac{\partial h}{\partial y}+\frac{\partial}{\partial y}\left(\mu u\frac{\partial u}{\partial y}\right)+(1+j)K_B\mu u\frac{\partial u}{\partial y} \qquad (16)$$
$$-K_B\frac{\partial}{\partial y}(\mu u^2)$$

It should be noted that the governing equations presented here are more complete than those given, for example, in Ref. 20, in that all terms ranging from order unity to order $(Re_s)^{-1}$ appear. Although Ho and Probstein state that they have considered all terms ranging from order unity to order $(\epsilon Re_s)^{-1}$, actually one term of order $(\epsilon Re_s)^{-1}$ seems to be missing in their energy equation. However, this introduces no error in their computations since the missing term vanishes identically at the stagnation point.

State:

$$\rho = \rho(h,\ p) \qquad (17)$$

Viscosity Law:

$$\mu = \mu(h,\ p) \qquad (18)$$

At this point then, there are six unknowns u, v, h, p, ρ and μ which may be determined by solving the six equations, (13) through (18), simultaneously.

III. BOUNDARY CONDITIONS

The location of the edge of the viscous layer within the shock layer, and the magnitude of the physical variables at the outer edge of the viscous layer are not known "a priori". Therefore, for convenience, it was decided to integrate the governing equations from the wall to the shock wave, where the physical variables can be calculated.

It was assumed that the shock in the stagnation region is a surface of discontinuity concentric with the body. It was further assumed that thermochemical equilibrium is achieved behind the shock. Use of the Rankine-Hugoniot relations yield the outer boundary conditions behind the shock wave:

$$u(x, \delta_s) = K_B x V_\infty \tag{19}$$

$$v(x, \delta_s) = (1 - \frac{1}{2} K_B^2 x^2)\, \epsilon\, V_\infty \tag{20}$$

$$p(x, \delta_s) = (1 - K_B^2 x^2)\,(1 - \epsilon)\, \rho_\infty V_\infty^2 \tag{21}$$

$$h(x, \delta_s) = (1 - K_B^2 x^2)\,(1 - \epsilon^2)\, \frac{V_\infty^2}{2} \tag{22}$$

where

$$\epsilon = \frac{\rho_\infty}{\rho_s} \tag{23}$$

It was also assumed that there is no slip or temperature jump at the wall and hence the boundary conditions at the wall are:

$$u(x, 0) = u_w = 0 \tag{24}$$

$$v(x, 0) = v_w \tag{25}$$

$$h(x, 0) = h_w \tag{26}$$

Note that the number of boundary conditions, namely seven, equals the order of the mathematical system.

Although the magnitude of the physical variables can be calculated behind the shock, the distance from the wall to the shock is not known. However, one may

introduce a constraint on the family of solutions based on the conservation of mass which takes the form:

$$\rho_\infty V_\infty r_s^{1+j} + \rho_w v_w r_w^{1+j} = \int_0^{\delta_s} \rho u (2r)^j dy \qquad (27)$$

This equation which serves to delimit the thickness of the shock layer δ_s is based on the fact that the gas flow between the body and the shock wave is the sum of the flow which enters the shock layer from the upstream side of the shock wave plus the gas injected at the surface.

IV. SEPARATION OF VARIABLES

The governing partial differential equations may be solved by means of the technique known as separation of the variables, which has previously proven useful in treating the low Reynolds number viscous layer, (Refs. 1, 17, 20, 21). In the manner suggested by Probstein and Kemp (Ref. 17) the following separable forms of the dependent variables were assumed which are compatible with the boundary conditions at the shock wave.

$$u = K_B x u_1(y) \tag{28}$$

$$v = (1 - \frac{1}{2} K_B^2 x^2)\, v_1(y) \tag{29}$$

$$h = (1 - K_B^2 x^2) h_1(y) - K_B^2 x^2 h_2(y) \tag{30}$$

$$\rho = (1 - \frac{1}{\gamma} K_B^2 x^2)\, \rho_1(y) \tag{31}$$

$$p = (1 - K_B^2 x^2)\, p_1(y) - K_B^2 x^2 p_2(y) \tag{32}$$

$$\mu = (1 - \frac{\gamma-1}{2\gamma} K_B^2 x^2)\, \mu_1(y) \tag{33}$$

$$r = x(1 + K_B y) \tag{34}$$

where the terms with subscripts 1 or 2 are functions of y alone. For convenience, the following non-dimensional forms are introduced:

$$\bar{u} = \frac{u_1}{V_\infty}\,,\ \bar{v} = \frac{u_1}{\epsilon V_\infty}\,,\ \bar{h}_1 = \frac{h_1}{V_\infty^2/2}\,,\ \bar{h}_2 = -\frac{h_2}{V_\infty^2/2}$$

$$\bar{\rho} = \epsilon \frac{\rho_1}{\rho_\infty}\,,\ \bar{p}_1 = \frac{p_1}{\rho_\infty V_\infty^2}\,,\ \bar{p}_2 = \frac{p_2}{\rho_\infty V_\infty^2} \tag{35}$$

$$\bar{\mu} = \frac{\mu_1}{\mu_s Re_s}\,,\ \bar{y} = K_B y$$

where the subscripts ∞ and s refer respectively to the free stream conditions and to the state immediately behind the shock. Note that the Reynolds number is defined by:

$$Re_s = \frac{\rho_\infty V_\infty}{K_B \mu_s} \tag{36}$$

For convenience, a compressibility transformation is also introduced, i. e.

$$\eta = \int_0^{\bar{y}} \bar{\rho}\, d\bar{y} \tag{37}$$

With the above simplifications, the low Reynolds number viscous layer equations reduce to the following system of dimensionless non-linear ordinary differential equations with variable coefficients applicable for first order non-similar solutions in the forward region of a hypersonic vehicle:

$$(\bar{\rho}\bar{v})' + (1 + j)\left(\frac{\bar{u}}{\epsilon} + \bar{v}\right) = 0 \tag{38}$$

$$\bar{u}\left(\frac{\bar{u}}{\epsilon} + \bar{v}\right) + \bar{\rho}\bar{v}\bar{u}' - 2\frac{\bar{p}_1 + \bar{p}_2}{\rho} = (\bar{\rho}\bar{\mu}\bar{u}')' + (2 + j)\,\bar{\mu}\bar{u}' - (\bar{\mu}\bar{u})' \tag{39}$$

$$\epsilon\bar{\rho}\bar{v}\bar{v}' + \bar{p}_1' = \frac{4}{3}\,\epsilon(\bar{\rho}\bar{\mu}\bar{v}')' + (1+j)\left[\bar{\mu}\bar{u}' - \frac{2}{3}(\bar{\mu}\bar{u})'\right] \tag{40}$$

$$\bar{p}_2' + \bar{u}\left(\frac{\bar{u}}{\epsilon} + \bar{v}\right) = 0 \tag{41}$$

$$\mathrm{Pr}\,\bar{\rho}\bar{v}\bar{h}_1' = (\bar{\rho}\bar{\mu}\bar{h}_1')' + (1 + j)\,\bar{\mu}\bar{h}_1' \tag{42}$$

$$\bar{\rho}\bar{v}\bar{h}_2' + 2\left[(\bar{\rho}\bar{\mu}\bar{u}\bar{u}')' + (1 + j)\,\bar{\mu}\bar{u}\bar{u}' - (\bar{\mu}\bar{u}^2)'\right] \tag{43}$$

$$= \left(\frac{\bar{\rho}\bar{\mu}}{\mathrm{Pr}}\bar{h}_2'\right)' + (1 + j)\frac{\bar{\mu}}{\mathrm{Pr}}\bar{h}_2' + 2\frac{\bar{u}}{\epsilon}\left[\bar{u}^2 + \epsilon\bar{\rho}\bar{v}\bar{u}' - (\bar{h}_1 + \bar{h}_2)\right]$$

$$\bar{\rho} = \bar{\rho}(\bar{h}_1, \bar{p}_1) \tag{44}$$

$$\bar{\mu} = \bar{\mu}(\bar{h}_1, \bar{p}_1) \tag{45}$$

where the primes denote derivatives with respect to η. It is seen that separation of the variables has increased the number of unknowns to eight, including $\bar{u}$, $\bar{v}$, $\bar{h}_1$, $\bar{h}_2$, $\bar{p}_1$, $\bar{p}_2$, $\bar{\rho}$, $\bar{\mu}$. This requires that the number of governing equations also be eight, equations (38) to (45), while the overall order of the mathematical system is ten requiring ten boundary conditions.

The boundary conditions become:

At the surface, $\eta = 0$, equations (24), (25) and (26) yield

$$\bar{u}_w = 0,\ \bar{v}_w = \bar{v}_w, \tag{46}$$

$$\bar{h}_{1_w} = \bar{h}_w = -\bar{h}_{2_w} \quad \text{(isoenthalpic wall)}$$

At $\eta = \eta_s$, equations (19) through (22) yield:

$$\bar{u}_s = 1,\ \bar{v}_s = -1,\ \bar{h}_{1_s} = (1-\epsilon^2),\ \bar{h}_{2_s} = 0,\ \bar{p}_{1_s} = (1-\epsilon),\ \bar{p}_{2_s} = 0 \qquad (47)$$

The constraint equation becomes:

$$(1+\bar{\delta}_s)^{1+j} + \bar{\rho}_w \bar{v}_w = \int_0^{\bar{\delta}_s} \frac{\bar{u}}{\epsilon} \left[2(1+\bar{y})\right]^j d\eta \qquad (48)$$

Here it is noted that for the special case of zero mass transfer, i.e., $\rho_w v_w = 0$, examination of eq. (38) indicates that the constraint

$$\bar{v}'_w = 0 \qquad (49)$$

becomes identical with eq. (48). This latter result (Ref. 1) follows from the fact that since $\bar{u}_w$ and $\bar{v}_w$ are both zero (for zero mass transfer), unless $\bar{v}'_w$ also vanishes, one obtains the physically untenable result of an infinite density gradient at the wall, (Ref. 20).

In general, the transport properties depend on both temperature and composition. However, since the diffusion equations have been uncoupled, the composition of the gas is not calculated explicitly, and so it is necessary to resort to further approximations. Constant Prandtl and Lewis numbers have already been introduced and hence the thermal conductivity and the diffusion coefficients are not required explicitly. Thus, only the viscosity coefficient remains to be evaluated.

It is assumed that the gas is in chemical equilibrium, or more explicitly that the state of the gas can be determined from a Mollier diagram (e.g., Ref. 27). That is, knowledge of two state functions (e.g., pressure and enthalpy) uniquely determines the others (e.g., temperature, composition, density, etc.). As already noted it is assumed here that the viscosity coefficient can be approximated by Sutherland's formula for air (Ref. 28)

$$\mu = \mu(T) = 1.16 \times 10^{-5} \left(\frac{717}{225+T}\right)\left(\frac{T}{492}\right)^{3/2} \qquad (50)$$

with T in ^{o}R, μ is given in lb./ft. sec. However, since (from the Mollier diagram)

$$T = T(h,\ p) \qquad (51)$$

then implicitly

$$\mu = \mu(h, p) \tag{52}$$

and the equation of state may also be obtained from the Mollier diagram, i.e.,

$$\rho = \rho(h, p) \tag{53}$$

Conditions behind the shock were determined from shock tables which incorporate the 1959 ARDC model atmosphere, (Ref. 29).

V. DISCUSSION OF RESULTS

Solutions were obtained on an IBM 7094 high-speed digital computer in the hypersonic low Reynolds number viscous layer flight regime. Calculations were carried out for a range of flight speeds from 15,000 ft./sec. to 25,000 ft./sec., an altitude range from 150,000 ft. to 350,000 ft. for Reynolds numbers which were varied between 25 and 15,000 and a mass transfer parameter, $-0.4 \leq f_w \leq 0$. These results were then compared with earlier theoretical studies in the continuum regime and in the low Reynolds number viscous layer regime.

The non-dimensional system of equations, (38) to (45), was integrated from the wall out to the shock wave. Since the boundary conditions are split, it is necessary to employ an iterative procedure. Some typical solutions for the viscous shock layer profiles of $\overline{u}$, $\overline{v}$, $\overline{h}$ and $\overline{p}$ are shown in Figures 3 to 6. As indicated by previous studies, the viscous effects extend further into the shock layer with decreasing Reynolds number.

After numerous calculations for a wide range of altitudes, flight speeds, Reynolds numbers, wall temperature, and mass transfer rates, it was found that all of the data could be correlated with several standard non-dimensional ratios as functions of the Reynolds number in combination with the shock density ratio.

All of the results of this study were normalized with respect to boundary layer predictions for precisely the same flight conditions and gas model. New boundary layer solutions for this study were obtained by retaining only first order terms in equations (38) to (45), thereby yielding the high Reynolds number asymptote. These boundary layer results are in reasonable agreement with those of other investigators, (Ref. 33). However, the discrepancies between the various predictions is nearly as large as the low Reynolds number effects. Thus, in order to assess the effects of low Reynolds number alone,we obtained these new boundary layer solutions which are completely compatible with our low Reynolds number solutions. The details of these calculations will appear in a paper to be presented shortly in which the hypersonic shock layer is examined over a region in which continuum concepts may reasonably be expected to be valid, i.e., from boundary layer concepts to merging of the shock with the fully viscous flow behind it.

All of the normalized heat transfer rates with no mass transfer obtained for the present investigation are shown in figure 7. Note that two values of the heat transfer rate are given for a particular value of $\epsilon^2 Re_s$. This is due to the assumed form of the mathematical separation of variables. Combining the two algebraically yields a first-order non-similar solution to the heat transfer rate partly around the body:

$$Q_{w_o} = \left(Q_{w_o}\right)_1 \cos^2(K_B x) + \left(Q_{w_o}\right)_2 \sin^2(K_B x) \tag{54}$$

and is valid for

$$\sin^2(K_B x) \leq 0(\epsilon) \tag{55}$$

For example, at an altitude of 150,000 ft., a flight speed of 15,000 ft./sec., $\epsilon \approx 0(0.1)$ and so $(K_B x)_{max} \approx 18.5^o$. It is seen that the concept of similarity is a reasonably good approximation at higher Reynolds numbers, in agreement with Ref. 34. However, when the viscous effect are significant over a major portion of the shock layer, this assumption becomes less reasonable, which is not in agreement with Ref. 34. However, since the results of the present study are only valid in the larger Reynolds number range of the low Reynolds number regime (i.e., viscous layer subregime) not much else can be said here concerning the discrepancy.

It was found that plotting all of our normalized heat transfer rate results with respect to the parameter $\epsilon^2 Re_s$ reduced the scatter to a minimum. Furthermore, it reduced the discrepancies between various theoretical and experimental studies previously conducted (Refs. 1, 20, 23, 30, 31, 35 and 36). It is seen that the results of the present analysis indicate the same general trends but a somewhat larger magnitude than all of these earlier studies with the exception of that of Ferri, et. al. (Ref. 30) which is almost identical with our present results. Coincidently, only in Ref. 30 and in the present study was a self consistant boundary layer asymptote determined in order to separate the low Reynolds number effects. However, it should also be noted that the results of Ref. 30 do not increase with decreasing Reynolds number as rapidly as the present more complete analysis indicating the need to retain more higher order terms with decreasing Reynolds numbers. This is further demonstrated by the results of

Kao (Ref. 35), i.e., the divergence of his second-order boundary layer and third-order boundary layer predictions at small Reynolds numbers, and comparison with Ho and Probstein's results (Ref. 20). It is noted that the conditions, gas model and boundary layer asymptote are the same in both of these references.

It is stressed that the calculations in this study were carried out down to values of Re_s, $\epsilon^2 Re_s$ and $\epsilon^3 Re_s$ below the range in which it is expected that the viscous layer will merge with the shock wave, in order to distinguish between the various predictions. From Refs. 20 and 30, it would appear that the lower limit of the viscous layer regims is of the order of $Re_s = 100$. Ho and Probstein (Ref. 10) extended their viscous layer results into the merged viscous layer regime by modifying a previous study (Ref. 17, constant density solution). In a more recent study by Levinsky and Yoshihara (Ref. 21), the same system of equations and perfect gas model employed by Probstein but utilizing a different gas, was solved from the free stream through the merged shock and viscous layer to the wall. Their results are naturally similar, except that paradoxically they are shifted by more than an order of magnitude to higher Reynolds numbers (see Ref. 1). However, the peak in their results with a downward trend at the lower Reynolds numbers indicates the merged shock layer structure. As noted earlier, Cheng (Ref. 22) did not make the poor assumption of a perfect gas shock structure, but modified the Rankine-Hugoniot shock relations to account for the normal components of the energy and momentum transfer through the shock wave. His results are also shown in figure 7.

It is, of course, expected that a realistic merged viscous layer analysis will yield results which will show a downward trend, somewhat similar to Cheng's, and will not continue to increase with decrease in $\epsilon^2 Re_s$ as the various viscous layer models indicate in figure 7.

Recent experimental results obtained by Hacker and Wilson (Ref. 31) are also shown in figure 7 utilizing their correlation relation

$$\frac{Q}{(Q)_{BL}} = 1 + \frac{0.4 \pm 0.1}{\sqrt{Re_s}} \tag{56}$$

and assuming $\epsilon = 0.12$. Only minor low Reynolds number effects are indicated,

whereas Ferri, et. al.'s (Ref. 30) experimental results appear to justify their own theory indicating a more significant low Reynolds number effect. The more recent experimental results of Vidal and Wittliff (Ref. 36) also agree well with those in Ref. 30 indicating the more significant low Reynolds number effect.

The numerical discrepancies between the results of the present study and those obtained earlier by us (Ref. 1) is mainly due to the method of calculation. The results in Ref. 1 were obtained on an analog computer, whereas, the present results were obtained in a more exact fashion on an IBM 7094 digital computer which is inherently more accurate than any analog computer.

Normalized skin friction results of this investigation are compared with some others reported on in the open literature in figure 8. It is seen in this figure that the present study shows a larger low Reynolds number effect than earlier studies.

It was shown in Ref. 1 that the gas model employed was naturally not as significant in the calculations of skin friction as for heat transfer rates. In fact, the low Reynolds number nature of the flow was shown to be the important criteria. Most of the terms neglected in the studies of Ho and Probstein (Ref. 20) appear in the equation for the x-component of momentum, which is most influential in the determination of the shear stress. This can also be seen by the discrepancies in the two predictions of Kao (Ref. 35) and Ho and Probstein (Ref. 20). It found that the abscissa $\epsilon^3 Re_s$ used in this figure reduced the scatter such that most of the calculations were right on the curve and the rest had a scatter of no more than two-three percent.

It has already been shown that in the absence of mass transfer it is convenient to normalize the heat transfer rate and surface shear stress by means of the high Reynolds number (boundary layer) asymptote. This suggests that when mass transfer is present one can again normalize the low Reynolds number results by means of the corresponding high Reynolds number asymptote. A summary of the effects of air injection into air at high Reynolds numbers from new boundary layer calculations is shown in figure 9, where the mass transfer parameter B is defined as

$$B = \frac{\dot{m}_w (H_s - h_w)}{Q_{w_o}} \qquad (57)$$

In figures 10 and 11 the normalized (i.e., normalized with respect to our new boundary layer solutions) contributions of the heat transfer are shown as a function of $\epsilon^2 Re_s$, wall temperature and dimensionless mass transfer rate f_w defined as

$$f_w = - \frac{\rho_w v_w}{\sqrt{(1 + j)\, \rho_w \mu_w \frac{du_s}{dx}}} \qquad (58)$$

It is seen that the effectiveness of the mass transfer process continues into the low Reynolds number regime, being somewhat less effective for a cool wall.

Interestingly the single curve for the present results of normalized skin friction shown in figure 9 represents not only the zero mass transfer cases but also all of our results with mass transfer.

As mentioned earlier, calculations at Reynolds numbers as high as 15,000 were carried out for this study. Our first attempts at normalization (using the boundary layer correlations of Scala and Gilbert, Ref. 37) indicated that at this high a Reynolds number the low Reynolds numbers effects on heat transfer and skin friction were quite small. However, there were discrepancies such that satisfactory correlations could not be achieved. Thus, it was decided to carry out a compatible boundary layer analysis. Using these new solutions we have been able to correlate all of the low Reynolds number results. However, it is now seen that even at this high a Reynolds number that there is a difference in the zero mass transfer heat transfer rate predictions of about ten percent and about thirty percent for the skin friction. It is, thus, seen that the low Reynolds number effects appear to extend to much higher Reynolds numbers than had previously been reported. This will be discussed in greater detail in another paper soon to be released.

In the high Reynolds number regime, the shock detachment distance is a function of body shape, density and velocity, independent of surface temperature and mass transfer at moderate rates of injection. However, at lower Reynolds numbers, the shock detachment distance is a function of body shape, flight speed, altitude, Reynolds number, wall temperature and mass transfer rate. This effect was investigated in order to predict the effects of mass transfer in the low Reynolds number viscous layer regime

upon shock wave detachment distance. Figure 12 shows the variation of δ_s/R_B with the above parameters at a single flight speed and two wall temperatures. Intuitively, one expects that due to the extended interaction region, mass injection will push the shock wave further away from the body with decreasing Reynolds numbers. As shown in figure 12, this is indeed found to be the case.

As noted earlier, the location of the "edge" of the boundary layer within the shock layer is not known "a priori". However, "a posteriori" the limit of the viscous effects δ_{BL}/R_B can be defined as the location at which $\rho_e/\rho = 0.995$. Using this definition, δ_{BL}/R_B for the same conditions is also shown in figure 12. The terminus at the lowest Reynolds number is the intersection of the edge of the boundary layer with the shock detachment distance. Obviously, this theory fails at a somewhat higher Reynolds number since the shock wave has also thickened appreciably before merging with the viscous layer. Also shown is the estimate based on our new boundary layer solutions. It is seen that even at the large value $Re_s = 15,000$ the boundary layer thickness prediction is greater for boundary layer analysis.

VI. CONCLUSIONS

1) Useful correlations for heat transfer and skin friction have been obtained for the hypersonic low Reynolds number viscous layer.

2) The effects of mass transfer of air molecules into the viscous layer have also been determined and correlated herein.

3) The range of applicability of the present model has been delimited.

ACKNOWLEDGMENTS

The authors are pleased to acknowledge the assistance of the scientific programming staff of the Theoretical Fluid Physics Section, in particular Messrs. Frank Bosworth and James Massey for programming the low Reynolds number equations and Stephen Schechner for programming the boundary layer equations.

This paper is based on work which was supported by the following United States Air Force Contracts AF 04(647)-617, AF 04(694)-473 and AF 04(694)-389.

REFERENCES

1. Goldberg, L. and Scala, S. M., "Mass Transfer in the Hypersonic Low Reynolds Number Viscous Layer", IAS Preprint 62-80, Presented at the IAS Thirtieth Annual Meeting, New York City, January 22, 1962.

2. Hayes, W. D. and Probstein, R. F., "Hypersonic Flow Theory", Academic Press, New York, 1959.

3. Lees, T., "Laminar Heat Transfer Over Blunt Bodies at Hypersonic Flight Speeds", Jet Propulsion, Vol. 26, pp. 259-269, 1956.

4. Fay, J. A. and Riddell, F. R., "Theory of Stagnation Point Heat Transfer in Dissociated Air", J. Aero. Sci., Vol. 25, pp. 78-85, 1958.

5. Scala, S. M., "A Study of Hypersonic Ablation", Proceedings of the Tenth International Astronautical Federation Congress, London, Springer Verlag, pp. 790-828, 1959.

6. Scala, S. M. and Ashley, W. F., "Mass Addition Effects on Hypersonic Heat Transfer to a Two-Dimensional Body", Proceedings of the 1961 International Heat Transfer Conference, Univ. of Colorado, Boulder, Colorado, pp. 696-706, 1961.

7. Gilbert, L. M. and Scala, S. M., "Free Molecular Heat Transfer in the Ionosphere", AAS Preprint 61-72, to appear in the Proceedings of the American Astronautical Society Symposium on Interactions of Space Vehicles with an Ionized Atmosphere, Washington, D. C., 1961.

8. Wachman, H. Y., "The Effect of Surface Properties on Energy Transfer at Low Gas Densities", Proceedings of General Electric Co., MSVD, High Altitude Aerodynamics Conference, Paper 2.3, 1961.

9. Wachman, H. Y., "Thermal Accomodation Coefficient: A Critical Survey", ARS Journal, Vol. 32, No. 1, p. 1, 1962.

10. Hartnett, J. P., "A Survey of Thermal Accomodation Coefficients", Proceedings of the Second Rarefied Gas Dynamics Symposium, Academic Press, pp. 1-28, 1960.

11. Willis, D. R., "A Study of Some Nearly Free Molecular Flow Problems", Pl. D. dissertation, Princeton University, Princeton, New Jersey, 1958.

12. Baker, R. M. L., Jr. and Charwat, A. F., "Transitional Correction to the Drag of a Sphere in Free Molecule Flow", Phys. Fluids, Vol. 1, pp. 73-81, 1958.

13. Enoch, J., "A Kinetic Model for Hypersonic Rarefied Gas Flow", General Electric Co., MSVD, TIS R61SD063, 1961.

14. Willis, D. R., "Methods of Analysis of Nearly Free Molecule Flow For a Satellite or Other Space Vehicle", General Electric Co., MSVD, TIS R60SD399.

15. Hamel, B. B., "A Model for the Transition Regime in Hypersonic Rarefied Gas Dynamics", AIAA Journal, Vol. 2, No. 6, June 1964.

16. Hoshizaki, H., "Shock-Generated Vorticity Effects at Low Reynolds Numbers", Lockheed Missiles and Space Division, LMSD 48381, Vol. 1, pp. 9-43, Jan. 1959.

17. Probstein, R. F. and Kemp, N. H., "Viscous Aerodynamic Characteristics in Hypersonic Rarefied Gas Flow", J. Aero. Sci., Vol. 27, pp. 174-192, 218, 1960.

18. Oguchi, H., "Blunt Body Viscous Layer With and Without a Magnetic Field", Phys. of Fluids, Vol. 3, pp. 567-580, 1960.

19. Hoshizaki, H., Neice, S. and Chan, K. K., "Stagnation Point Heat Transfer Rates at Low Reynolds Numbers", IAS Preprint 60-68, Presented at IAS Nat. Sum. Meet., June 28-July 1, 1960.

20. Ho, H. T. and Probstein, R. F., "The Compressible Viscous Layer in Rarefied Hypersonic Flow", Brown University, ARL TN 60-132, Aug. 1960. Also published in Proceedings of the Second Rarefied Gas Dynamics Symposium, Academic Press, pp. 525-552, 1960.

21. Levinsky, E. S. and Yoshihara, H., "Rarefied Hypersonic Flow Over a Sphere", Presented at the ARS International Hypersonics Conference, MIT, Cambridge, Massachusetts, 1961.

22. Talbot, L. and Scala, S. M., "Shock Wave Structure in a Relaxing Diatomic Gas", Proceedings of the Second International Symposium on Rarefied Gas Dynamics, Berkeley, California, pp. 603-622, 1960.

23. Cheng, H. K., "Hypersonic Shock-Layer Theory of the Stagnation Region at Low Reynolds Number", Proceedings of the 1961 Heat Transfer and Fluid Mechanics Institute, Stanford University Press, Stanford, California, 1962.

24. Sedov, L. I., Michailova, M. P. and Chernyi, G. G., "On the Influence of Viscosity and Heat Conduction on the Gas Flow Behind a Strong Shock Wave", Vestnik Moskovskovo Unversiteta, No. 3, p. 95, 1953.

25. Li, T. Y. and Geiger, R. E., "Stagnation Point of a Blunt Body in Hypersonic Flow", J. Aero. Sci., Vol. 24, pp. 25-32, 1957.

26. Hirshfelder, J. O. and Curtiss, C. F. and Bird, R. B., "Molecular Theory of Gases and Liquids", John Wiley and Sons, Inc., 1954.

27. Moeckel, W. E. and Weston, K. C., "Composition and Thermodynamic Properties of Air in Chemical Equilibrium", NACA TN 4265, 1958.

28. Jeans, J. H., "The Dynamical Theory of Gases", Dover Publications, Inc., New York, 1954.

29. Cook, C. A., Gilbert, L. M. and Scala, S. M., "Normal Shock Wave Calculations in Air at Flight Speeds Up to 25,000 Ft./Sec.", General Electric Company, MSD, TIS R62SD76, November 1962.

30. Ferri, A., Zakkay, V. and Ting, L., "Blunt Body Heat Transfer at Hypersonic Speeds and Low Reynolds Numbers", J. Aero. Sci., Vol. 28, pp. 962-971, 1961.

31. Hacker, D. S. and Wilson, L. N., "Shock Tube Results for Hypersonic Stagnation Heating at Very Low Reynolds Numbers", Proceedings of the Symposium on Dynamics of Manned Lifting Planetary Entry, Oct. 1962, John Wiley and Sons, Inc., New York, 1963.

32. Scala, S. M., "Transpiration Cooling in the Hypersonic Laminar Boundary Layer", General Electric Co., MSVD, TIS 58SD215, March 1958.

33. Scala, S. M. and Baulknight, C. W., "Transport and Thermodynamic Properties in a Hypersonic Laminar Boundary Layer: Part 2, Applications", ARS Journal, Vol. 30, No. 4, pp. 329-336, 1960.

34. Kao, H. C., "Hypersonic Viscous Flow Near the Stagnation Streamline of a Blunt Body: I. A Test of Local Similarity", AIAA Jour., Vol. 2, pp. 1892-1897, 1964.

35. Kao, H. C., "Hypersonic Viscous Flow Near the Stagnation Streamline of a Blunt Body: II. Third-Order Boundary-Layer Theory and Comparison with Other Methods", AIAA Jour., Vol. 2, pp. 1897-1906, 1964.

36. Vidal, R. J. and Wittliff, C. E., "Hypersonic Low Density Studies of Blunt and Slender Bodies", Rarefied Gas Dynamics, Vol. II, (Ed. by J. A. Laurmann), Academic Press, New York, pp. 343-378, 1963.

37. Scala, S. M. and Gilbert, L. M., "Theory of Hypersonic Laminar Stagnation Region Heat Transfer in Dissociating Gases", General Electric Co., MSD, TIS R63SD40, April 1963. To be published in Developments in Mechanics, Ed. -S. Ostrach, Pergamon Press.

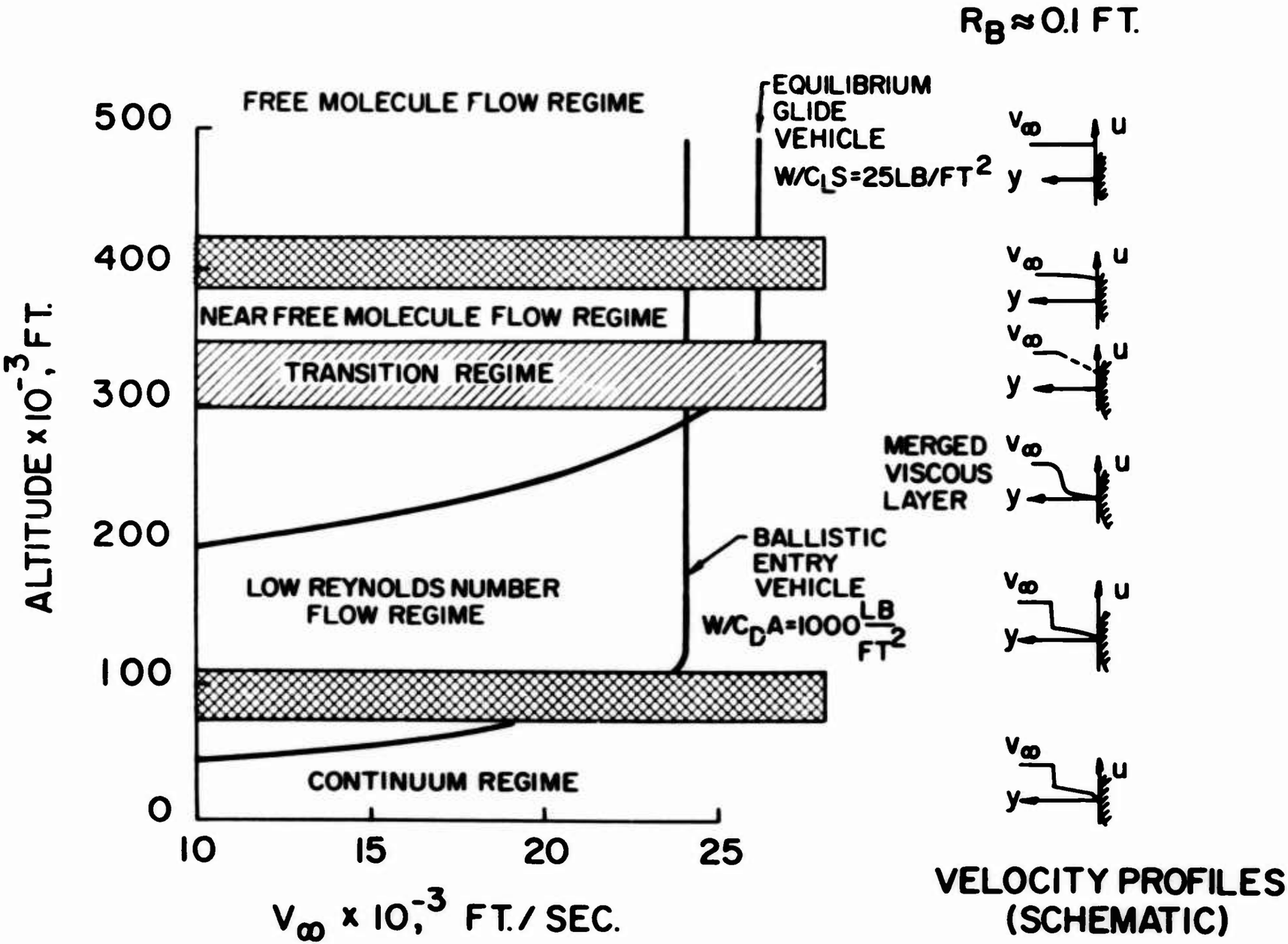

Figure 1. Hypersonic Flight Regimes

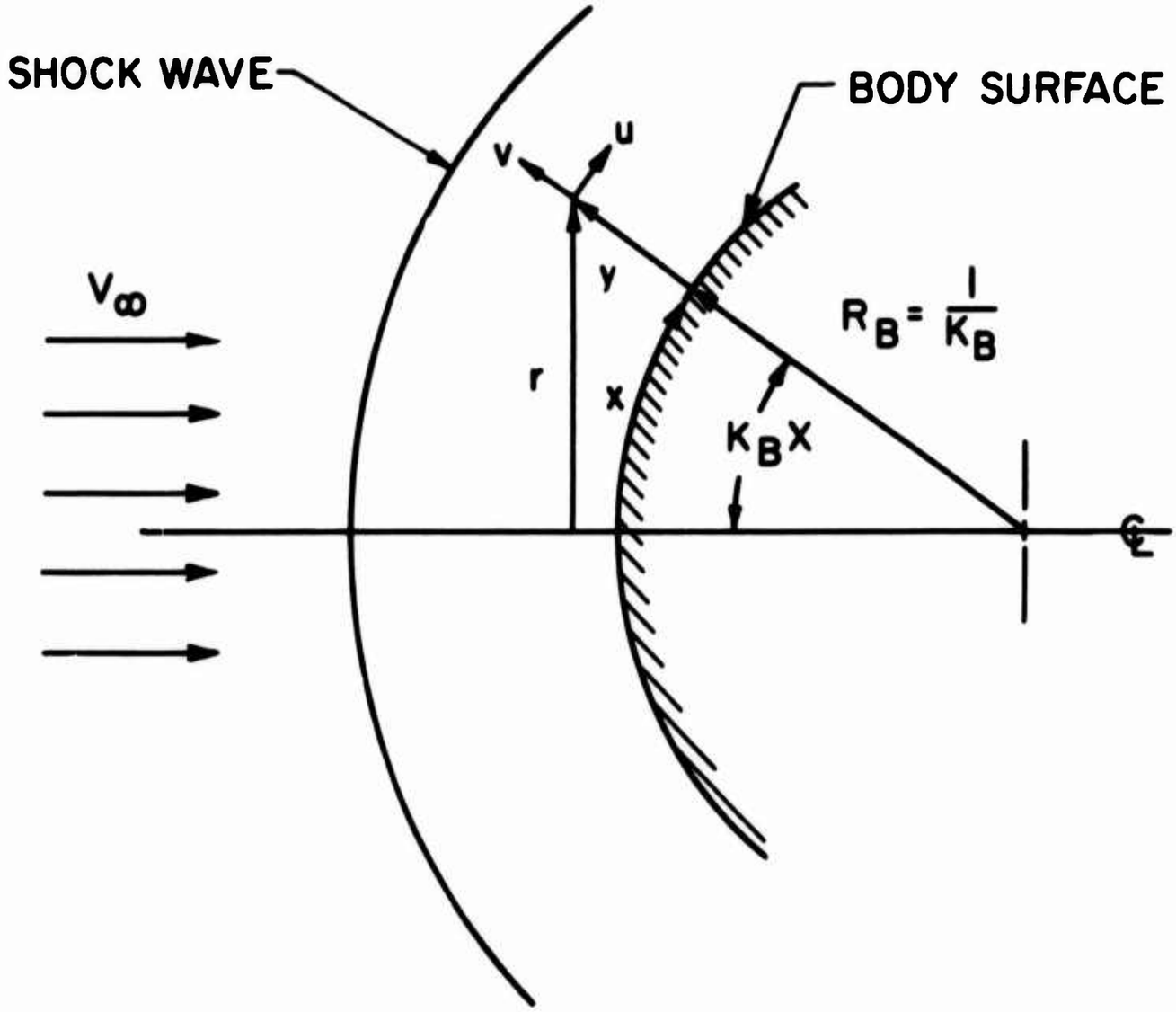

Figure 2. Coordinate System

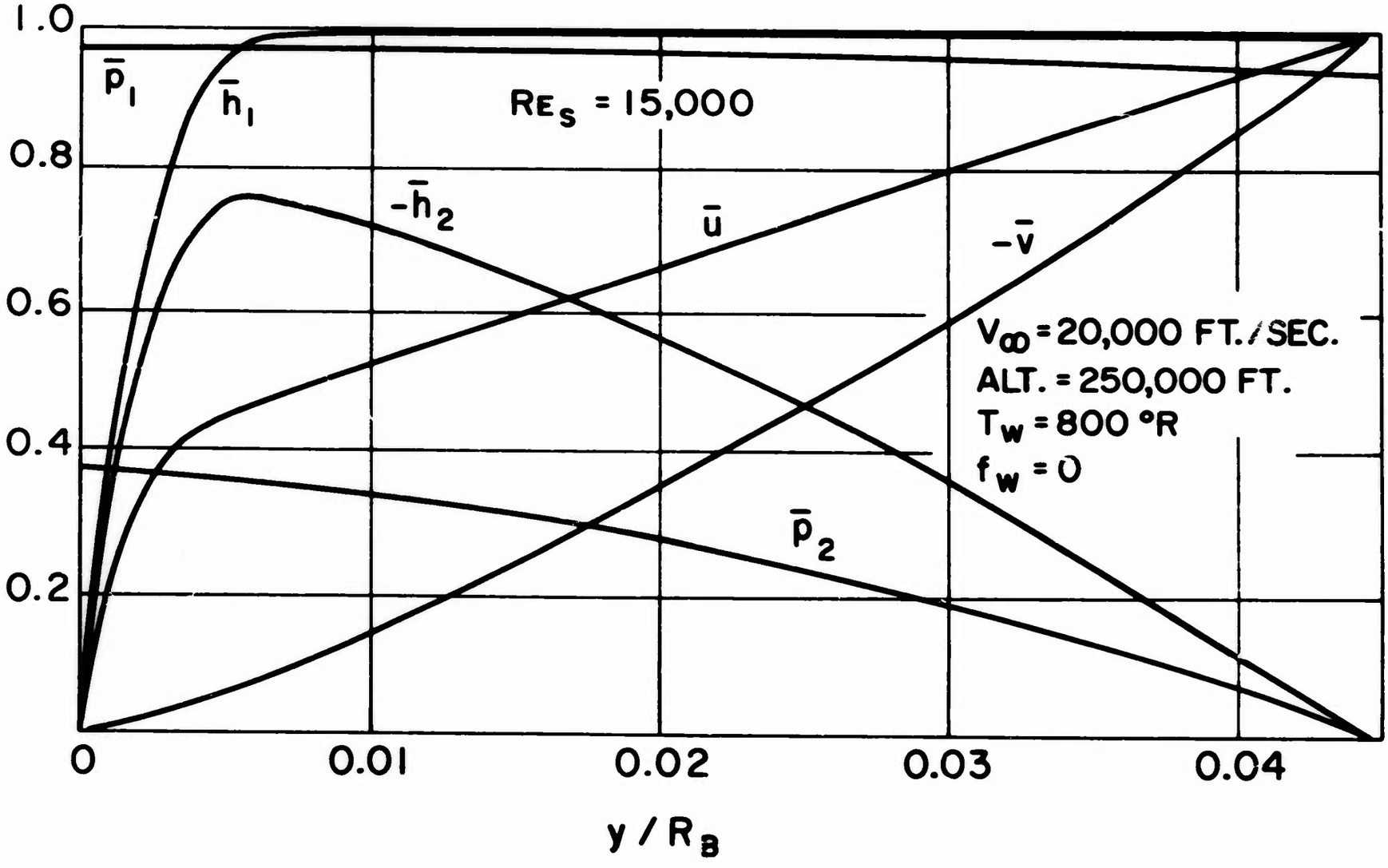

Figure 3. Profiles Re_s = 15,000

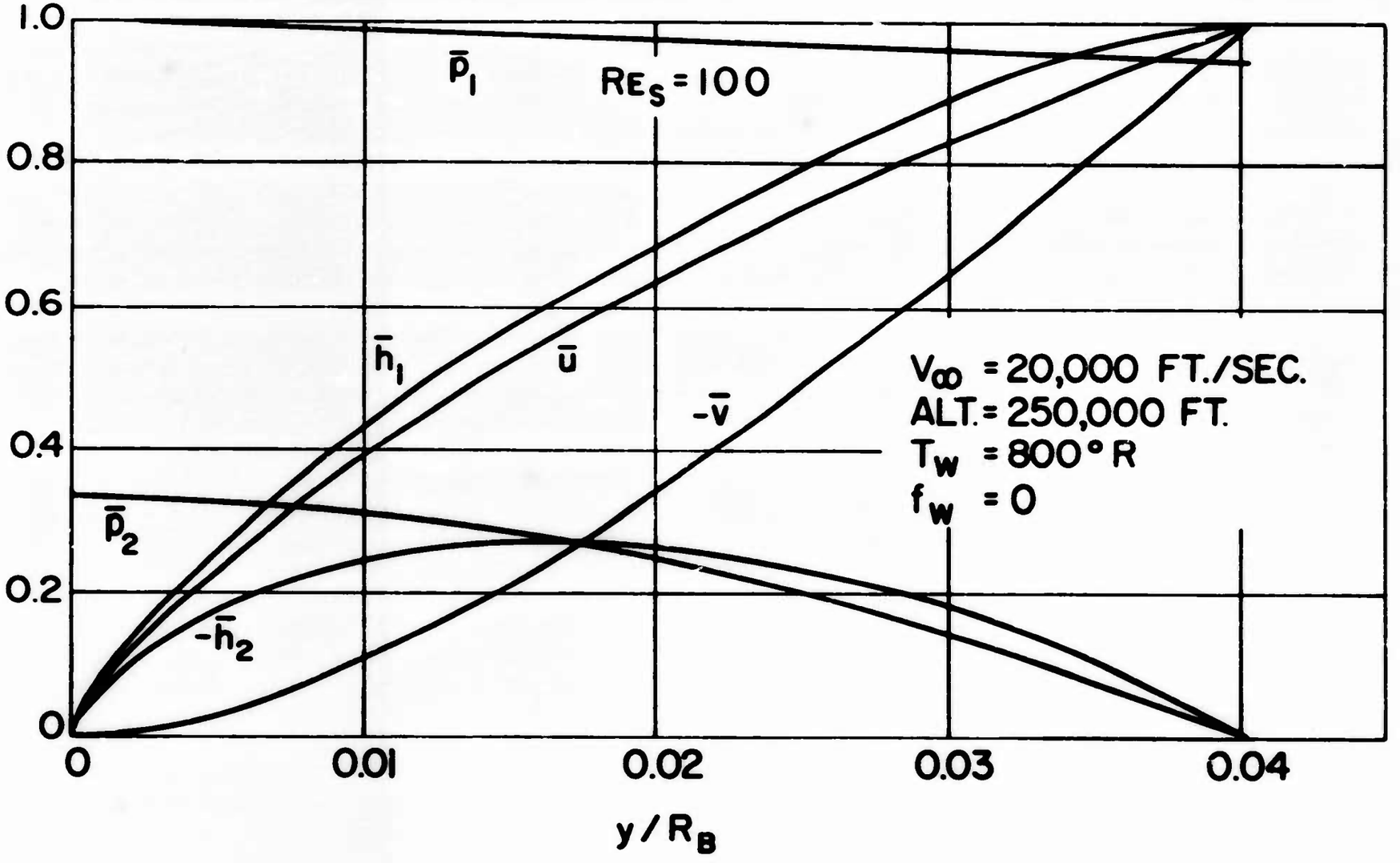

Figure 4. Profiles $Re_s = 10^3$

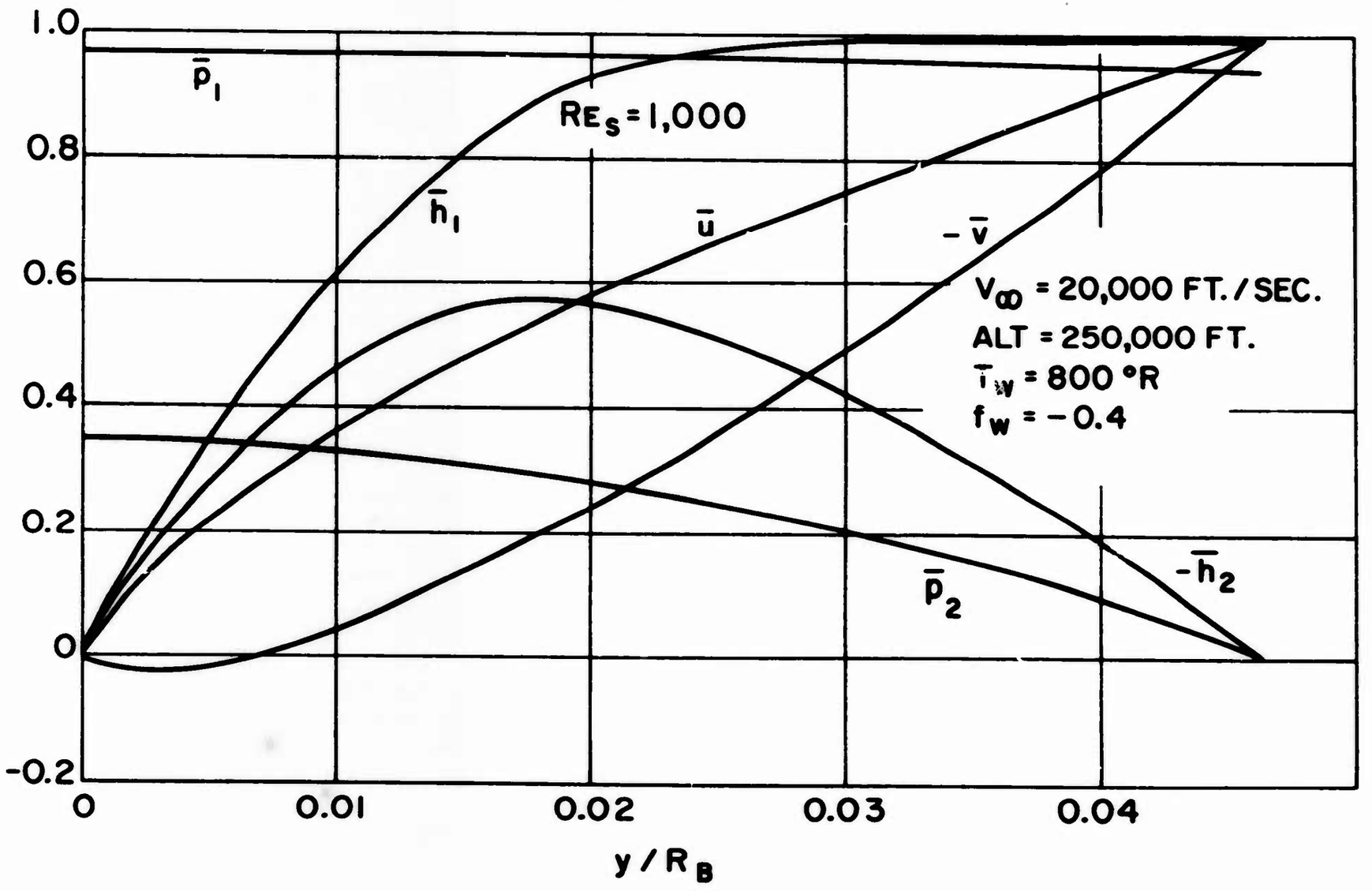

Figure 5. Profiles $Re_s = 10^3$, $f_w = -0.4$

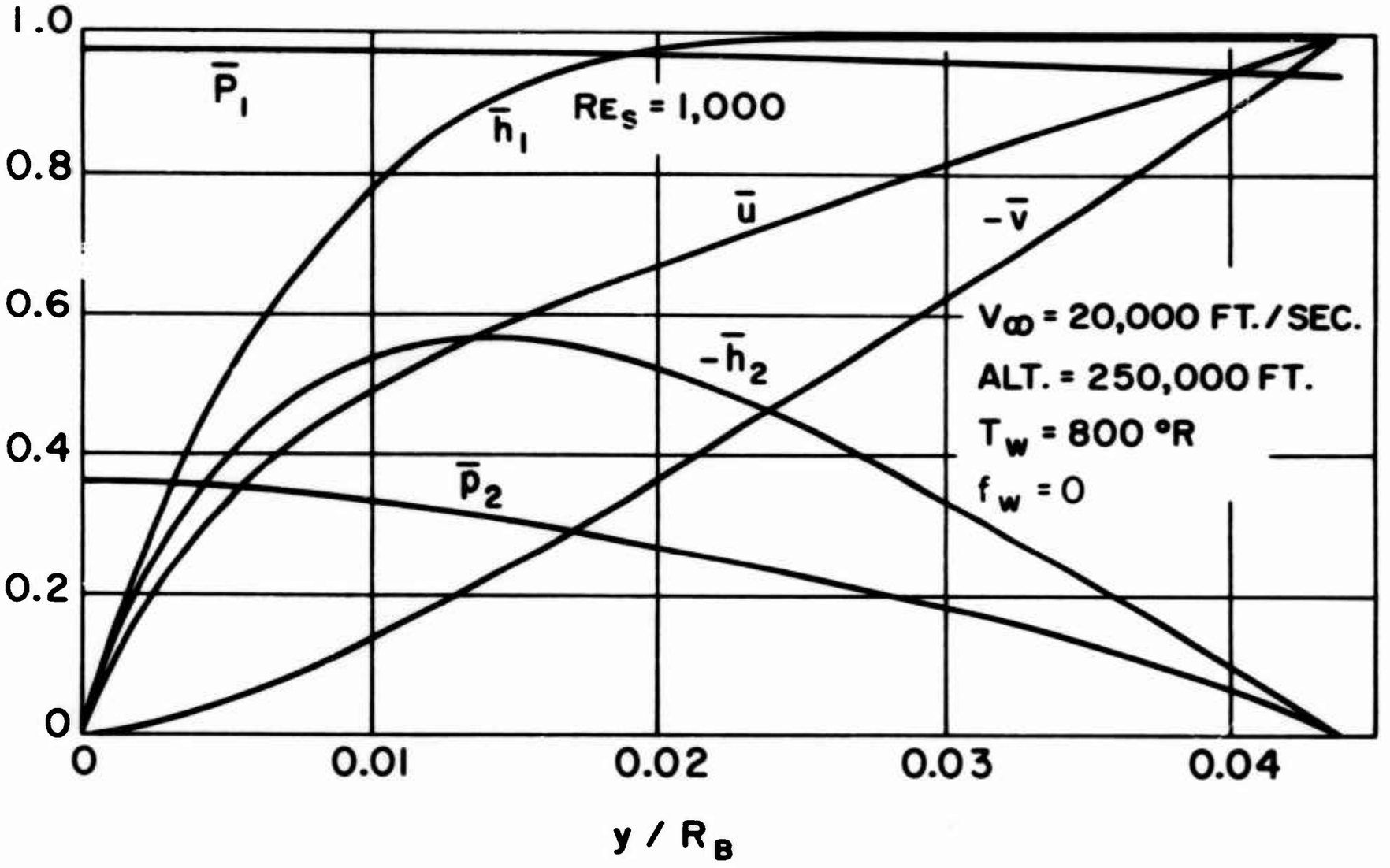

Figure 6. Profiles $Re_s = 10^2$

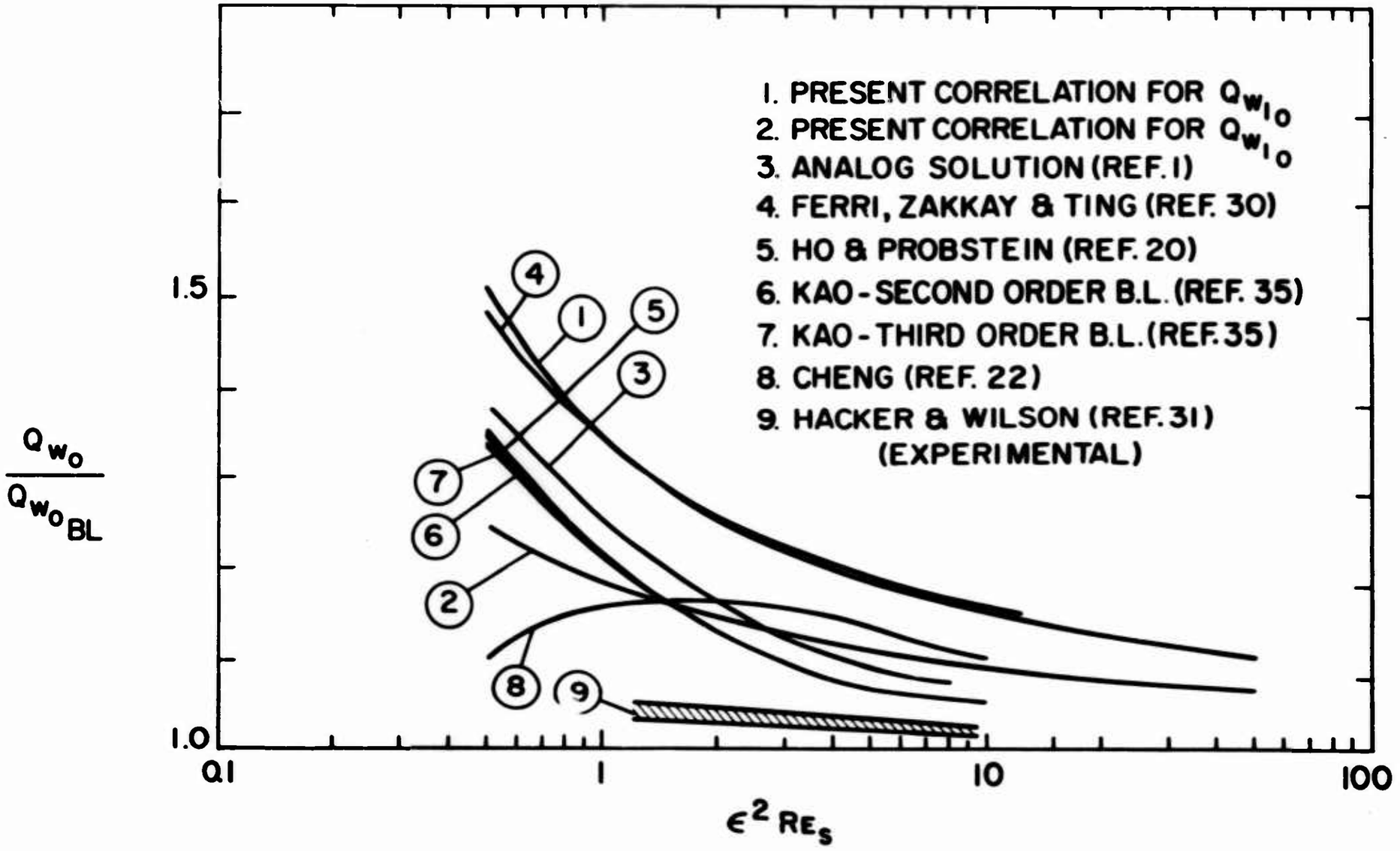

Figure 7. Normalized Heat Transfer

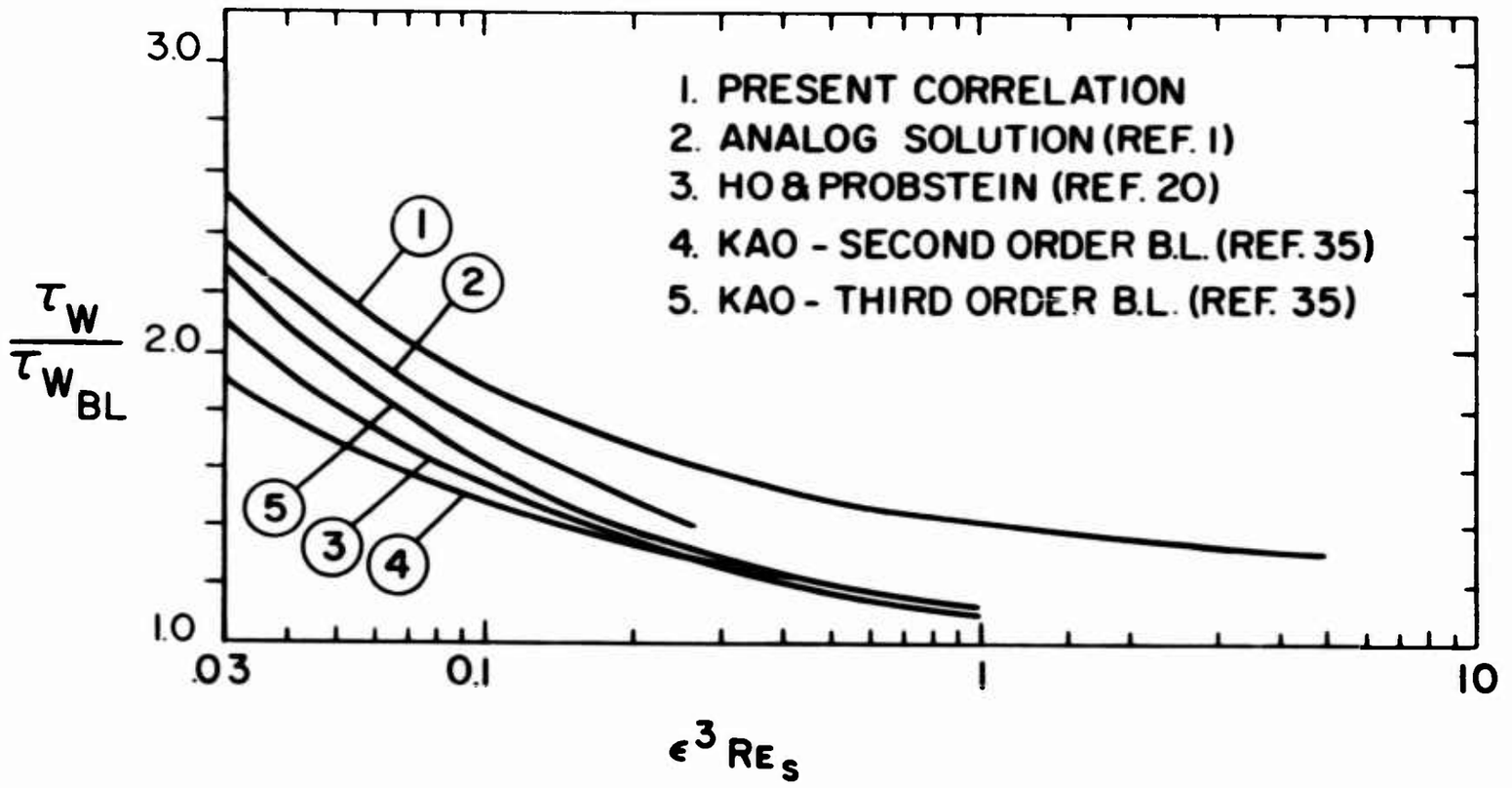

Figure 8. Normalized Skin Friction

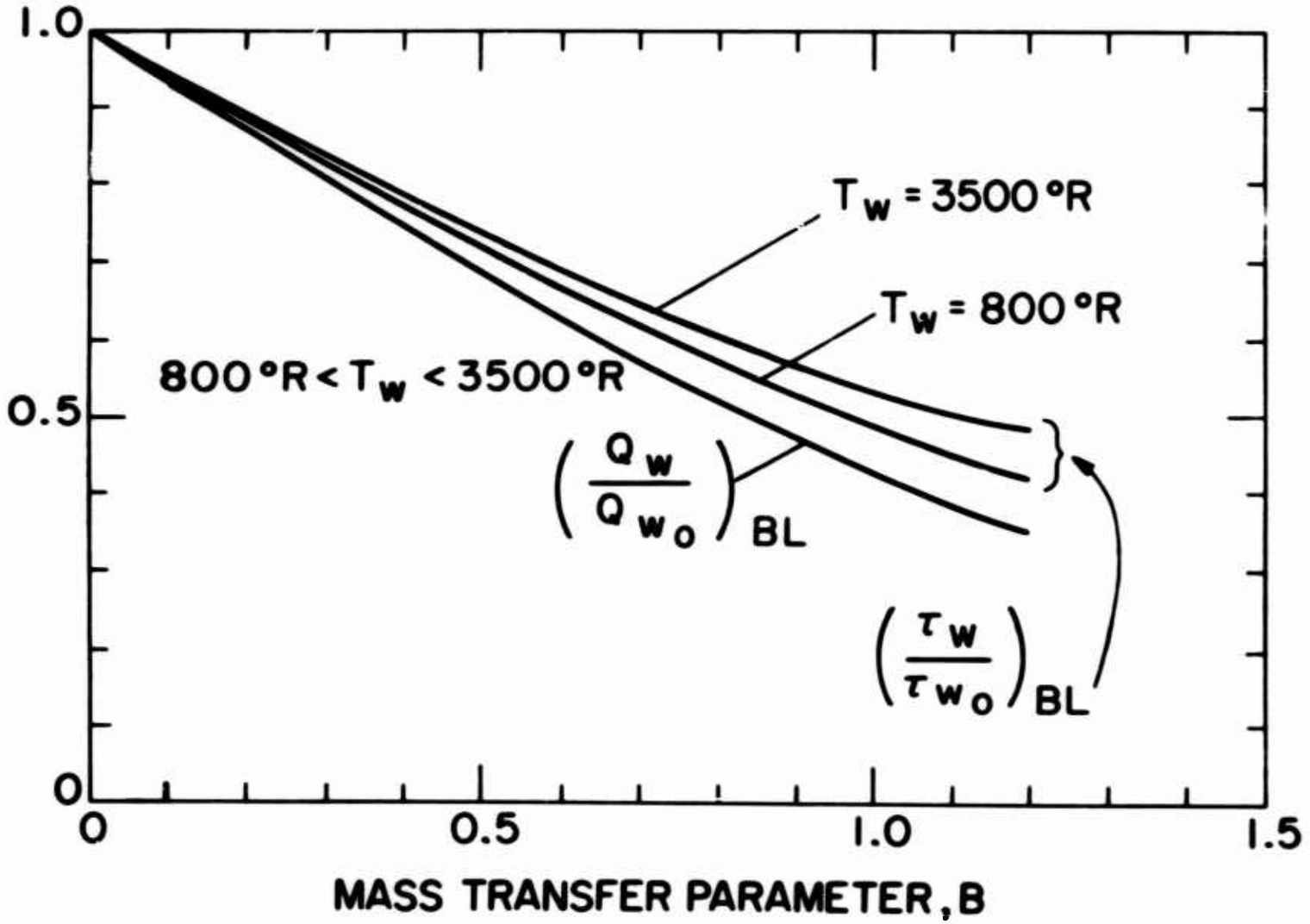

Figure 9. Boundary Layer Mass Transfer $(Q_w/Q_{w_o})_{BL}$ and $(\tau_w/\tau_{w_o})_{BL}$ vs B

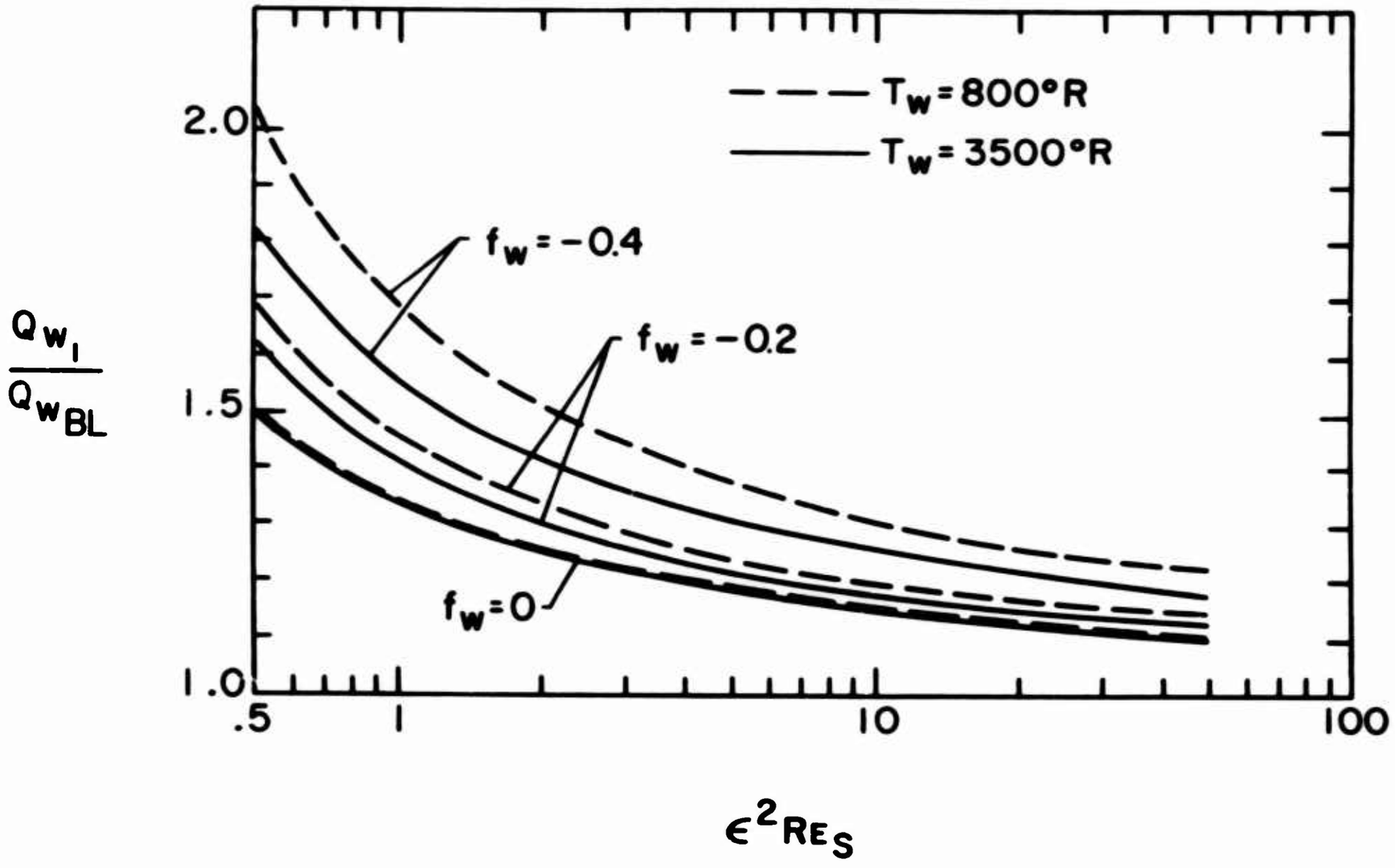

Figure 10. $(Q_{w_1})/(Q_w)_{BL}$ vs. $\epsilon^2 Re_s$ (Mass Transfer)

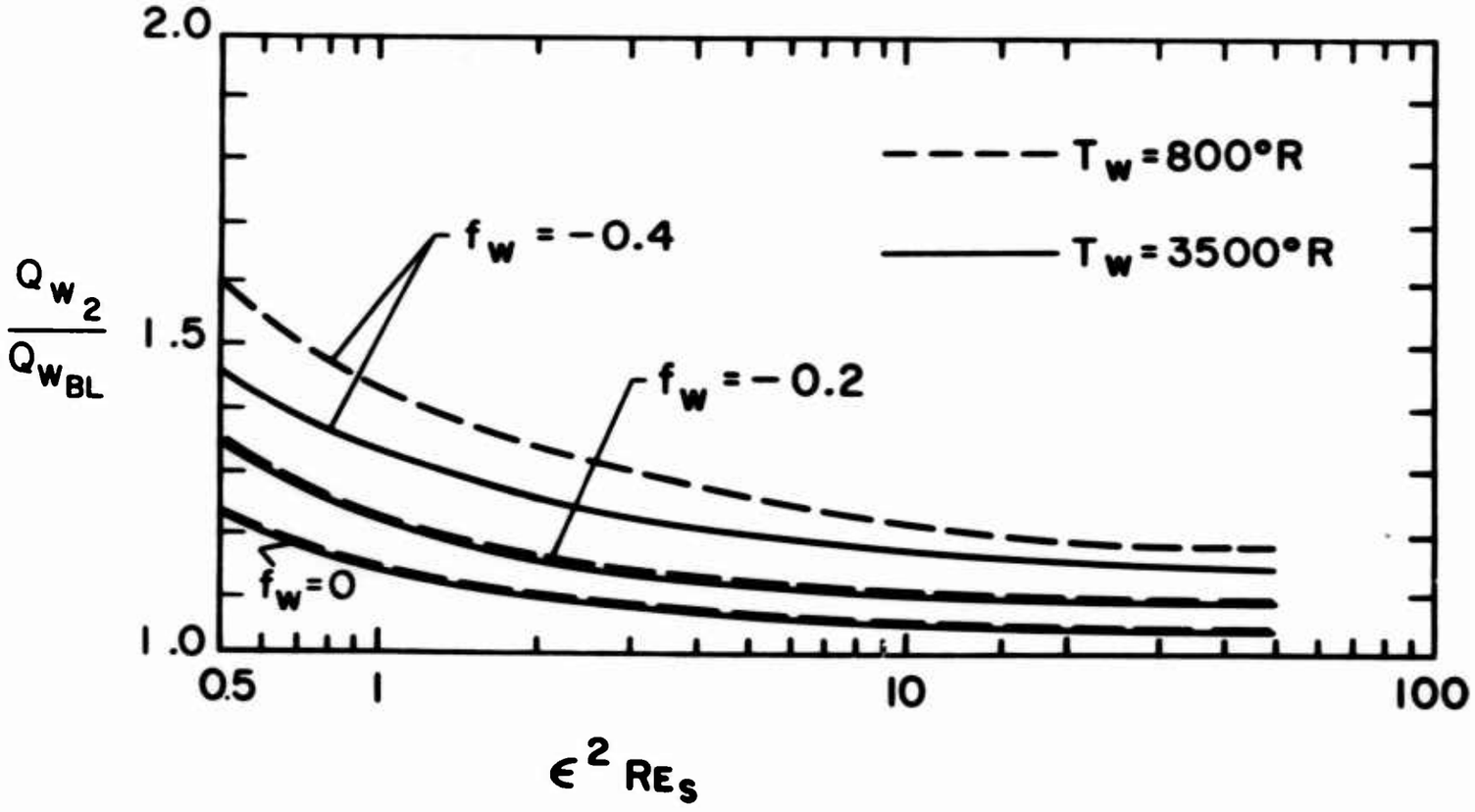

Figure 11. $(Q_{w_2})/(Q_w)_{BL}$ vs. $\epsilon^2 Re_s$ (Mass Transfer)

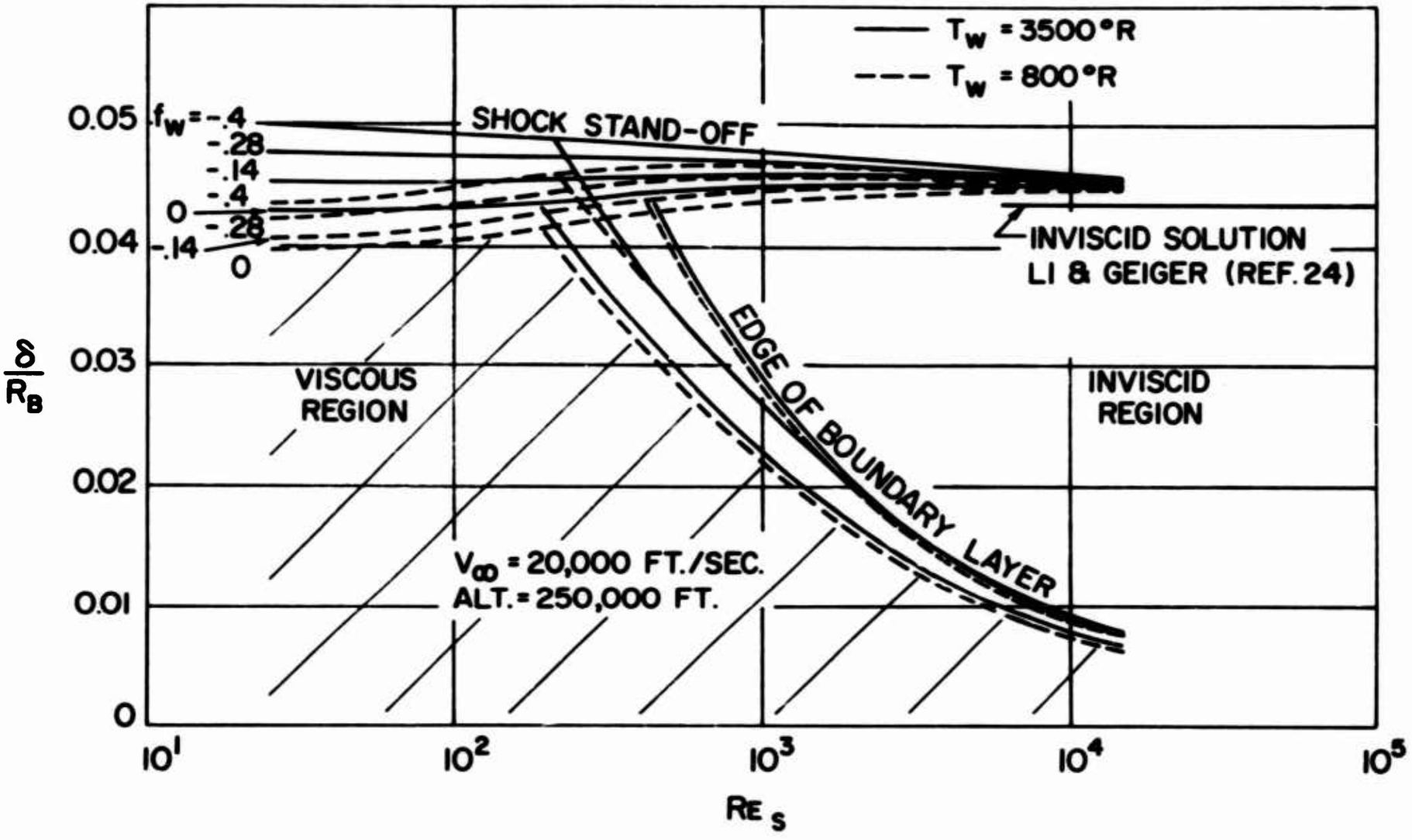

Figure 12. Shock Detachment and Viscous Layer vs Re_s

GENERAL ELECTRIC

SPACE SCIENCES LABORATORY
MISSILE AND SPACE DIVISION

TECHNICAL INFORMATION SERIES

AUTHOR	SUBJECT CLASSIFICATION	NO.
L. Goldberg S. M. Scala	Hypersonic Viscous Flow Heat Transfer Low Reynolds Number	R65SD27
		DATE July 1965
TITLE MASS TRANSFER IN THE LOW REYNOLDS NUMBER VISCOUS LAYER AROUND THE FORWARD REGION OF A HYPERSONIC VEHICLE		G. E. CLASS I
		GOV. CLASS Unclassified
REPRODUCIBLE COPY FILED AT MSD LIBRARY. DOCUMENTS LIBRARY UNIT. VALLEY FORGE SPACE TECHNOLOGY CENTER, KING OF PRUSSIA, PA.		NO. PAGES 36

SUMMARY

This paper describes a theoretical investigation of the effect of mass transfer into the hypersonic low Reynolds number viscous layer upon the heat transfer rate and skin friction, and represents an extension of an earlier study by the present authors. New results have been obtained and correlated as a function of the Reynolds number. The range of applicability of the present fluid dynamic model is also discussed and comparisons are drawn with earlier work, both theoretical and experimental.

KEY WORDS

Hypersonic; Low Reynolds Number; Heat Transfer; Skin Friction

BY CUTTING OUT THIS RECTANGLE AND FOLDING ON THE CENTER LINE, THE ABOVE INFORMATION CAN BE FITTED INTO A STANDARD CARD FILE

AUTHOR Leon Goldberg Sinclare M Scala

COUNTERSIGNED S M Scala S. M. Scala, Manager
Theoretical Fluid Physics Section